

See discussions, stats, and author profiles for this publication at: <https://www.researchgate.net/publication/45404909>

# Correspondence between Thermodynamics of Lattice Models and Real Substances at the Liquid–Gas Domain of the Phase Diagram

ARTICLE *in* THE JOURNAL OF PHYSICAL CHEMISTRY B · AUGUST 2010

Impact Factor: 3.3 · DOI: 10.1021/jp1022899 · Source: PubMed

---

CITATIONS

7

---

READS

29

## 2 AUTHORS:



**E. M. Apfelbaum**

Joint Institute for High Temperatures

**49** PUBLICATIONS **325** CITATIONS

SEE PROFILE



**Vladimir Sergeevich Vorob'ev**

Russian Academy of Sciences

**177** PUBLICATIONS **835** CITATIONS

SEE PROFILE

# Correspondence between Thermodynamics of Lattice Models and Real Substances at the Liquid–Gas Domain of the Phase Diagram

E.M. Apfelbaum\* and V. S. Vorob'ev

Joint Institute for High Temperatures of Russian Academy of Science, Izhorskaya 13, bldg. 2, Moscow 125412, Russia

Received: March 13, 2010; Revised Manuscript Received: June 18, 2010

We modify the projective transformation suggested earlier.<sup>7</sup> Within this modified transformation, the critical point and the Zeno-line of the lattice model are moved to the critical point and Zeno-line of simple liquids. Using analytical lattice calculations and numerical simulations, we show that the lattice binodals and critical isotherms transforms with sufficient accuracy into binodals and critical isotherms of real substances such as Cs, Hg, and NH<sub>3</sub>, and other model systems with real system properties such as the van der Waals equation, Lennard–Jones systems.

## Introduction

There is a continuing search for similarities and unifying principles in the description of a variety of thermodynamic properties of complex matter, which are the key points of statistical physics.<sup>1</sup> Different substances can exhibit general features, such as the principle of corresponding states or the law of rectilinear diameter. These features are referred to as the similarity laws. The Zeno-line (ZL) regularity has a special place among these laws because of the fact that, unlike other similarity laws, it is valid for a wider class of real substances. The ZL regularity law characterizes thermodynamic states of the system with compressibility equal to one,  $Z = P/(nk_B T) = 1$ . Here,  $P$  denotes the system pressure,  $n$  is the particle density,  $T$  is the system temperature, and  $k_B$  is the Boltzmann's constant. The states corresponding to ZL law form a straight line on the density–temperature plane.

In our previous works,<sup>2–5</sup> new regularities based on the ZL regularity were established. In particular, we showed that the ZL tends asymptotically to the liquid branch of binodal at low temperatures. Taking this fact into account and using only the three-term Guggenheim equation,<sup>6</sup> we constructed the temperature–density dependence for the liquid branch of binodal. Our method was sufficiently accurate for a very wide class of real materials. It was shown that the critical densities and temperatures of a very wide group of substances are also located along another straight line, which is parallel to ZL, with their parameters easily defined from the parameters of the ZL line. However, in all studies mentioned above the gas branch of the binodal was never analyzed.

In recent Kulinskii work,<sup>7</sup> a simple geometrical relations between the ZL and binodal curve have been used to consider for possible global isomorphism between the phase diagram of the lattice gas (LG), or equivalently, the Ising model, and the liquid–gas part of the diagram of a simple continuous fluid. Corresponding projective transformation between the lattice variables (density  $\rho$  and temperature  $t$ ) and real liquid variables (density  $n$  and temperature  $T$ ) have been also offered in ref 7. The ZL on the  $(\rho, t)$  plane is the vertical line  $\rho = 1$ , which is the tangent to lattice binodal curve. The transformation offered in ref 7 turns this vertical line into the ZL in the  $(n, T)$  plane.

The latter one is described by the equation:

$$n/n_B + T/T_B = 1 \quad (1)$$

The temperature  $T_B$  corresponds to the Boyle point, and  $n_B$  is the density obtained from the extrapolation the coexistence curve into the low temperature region beyond the triple point. The critical lattice density ( $\rho_c = 1/2$ ) and critical temperature ( $t_c = 1$ ) transform into the Zeno-median with following relation between the ZL parameters and the critical point:  $2n_c/n_B + T_c/T_B = 1$ . Thus, the relation is set up between the parameters of the ZL and the critical point. Geometrically this means that the critical point must lie on the Zeno-median in the  $(n, T)$  plane.<sup>7</sup> However, it is not always this case in general. The results of refs 2–5 indicate that the critical points in the  $(n, T)$  plane lie close to the line given by the equation  $n_c/n_B + T_c/T_B = 1 - a$ . The parameter  $a \approx 0.33$  for Lennard–Jones systems. Therefore, the critical points are located on the line parallel to the ZL line rather than on the Zeno-median.

In this work, we discuss the modification of the transformation reported in ref 7. We show that new transformation maps the point  $(1/2, 1)$  in the  $(\rho, t)$  plane with the point  $(n_c, T_c)$  in the  $(n, T)$  plane. Moreover, the correspondence between the ZL on these planes is conserved. Further, we analyze geometrical concepts of the correspondence between the liquid–gas domains of the phase diagram of the LG and simple fluids. For this purpose, we use different lattice models (LM) such as: the Bragg–Williams (BW) approach (ref 8), the quasi-chemical approach of Bethe–Guggenheim (BG) (ref 9), and recent computer simulations results,<sup>10,11</sup> and analytical predictions for 3D Ising model (ref 10).

We show that the LM binodals can be transformed into the binodals of certain continuous models which approximate real systems. The continuous models may include van der Waals and Lennard–Jones liquids, and other liquids such as cesium, mercury, and ammonia.

This article is organized as follows. The lattice models under study are described in section II. The section III is devoted to the theory of lattice binodal approximation. The lattice-to-continuous model transformation is presented in section IV. Sections V and VI contain the results of the binodal and critical

\* Corresponding author e-mail: apfel\_e@mail.ru.

isotherm calculations. The discussion of thermodynamic similarity is given in section VII. The conclusions are presented in section VIII.

## II. Lattice Models

Lattice models (LM) are usually based on a system of spins placed at the nodes of some particular lattice structure. In many cases, LM are obtained by means of simple discretization of corresponding continuum model, and thus exhibit structural properties similar to the latter. For example, in ref 12 it was demonstrated that “finely discretized lattice models for Lennard–Jones or Buckingham exponential-6 potential fluids have thermodynamic and structural properties essentially identical to their continuum counterparts”. In the current study, we consider the case of a cubic LM assuming that all spins are located on the cubic (square in 2D) lattice nodes. The lattice Hamiltonian  $H^{1,14}$  then reads:

$$H = - \sum_{\{i,j\}} J_{ij} s_i s_j - MB \sum_i s_i \quad (2)$$

Here,  $B$  is the magnetic field (hereafter is set to zero for simplicity,  $B = 0$ ),  $M$  is the average magnetic moment; spin values  $s_i = \pm 1$ ,  $J_{ij}$  is the interaction energy between different lattice sites  $i$  and  $j$ . We assume that all interactions but the interaction between the nearest-neighbor spins, are equal to zero.. This approximation is known as the standard Ising model. Hence, the summation in the first term of eq 2 is taken only over the nearest-neighbor sites and  $J_{ij} = J$ . The partition function for the Ising model is well known and was calculated analytically for 1D lattice by Ising, and for 2D lattice by Onsager (ref 1). Though no analytical solution exists for 3D case, several models based on different levels of approximations have been proposed. In most cases only a small part, or a cell in the whole 3D system is considered within these approximations. Then, making additional approximations for the interaction of the cell with the rest of 3D system, the behavior of the whole system is recovered using various extrapolation techniques. The interaction approximations usually invoke the following models – the mean-field Bragg and Williams (BW) model,<sup>8</sup> and the quasi-chemical Bethe-Guggenheim (BG) model<sup>9</sup> (also ref 1). These approximate models are simple and tractable, and predict qualitatively correct results for the system thermodynamics in the vicinity and around the critical point.

We first start with the case of BW approximation. In the framework of this theory, the chemical potential  $\mu$  and the pressure in the liquid can be written as

$$e^{\mu/T} = \frac{\rho}{1-\rho} e^{-Wc(2\rho-1)/T}; P/T = \ln\left(\frac{e^{-cW\rho^2/T}}{1-\rho}\right) \quad (3)$$

Here,  $T$  is the system temperature,  $\rho$  is the density,  $c$  is the number of the nearest-neighbor spin around the chosen node,  $W$  is the typical value for the interaction energy between neighboring spins. It follows from eq 3 that the critical parameters are

$$\rho_c = 1/2; W/T_c = 2/c \quad (4)$$

The binodals of the LM are symmetrical curves<sup>1</sup> in the  $(\rho, t)$  plane regarding to the straight line  $\rho = \rho_c = 1/2$ . The binodal equation is usually derived from eqs 3–4 using the symmetry

condition  $\mu(\rho) = \mu(1-\rho)$  or  $P(\rho) = P(1-\rho)$ . Implementing this condition, we arrive at

$$t = 2 \frac{2\rho - 1}{\ln\left(\frac{\rho}{1-\rho}\right)} \quad (5)$$

where  $t = T/T_c$  is the reduced temperature. It is evident that the binodal is independent of the number of neighboring sites  $c$ . In the limit of  $\rho \rightarrow 0$ , the eq 5 reduces to

$$\rho = \exp(-2/t) \quad (6)$$

The pressure in the reduced units becomes

$$p = P/P_c = \frac{t \ln(1-\rho) - 2\rho^2}{\ln(\frac{1}{2}) - \frac{1}{2}} \quad (7)$$

If  $\rho = 1/2$ , then eqs 4 and 5 give  $t = 1$  and  $p = 1$ .

Now, we consider the case of the quasi-chemical (or BG) approximation, which connects the density and chemical potential through a more complicated relation:

$$e^{\mu/T} = \left[ \frac{(\beta - 1 + 2\rho)(1-\rho)}{(\beta + 1 - 2\rho)\rho} \right]^{c/2} \frac{\rho}{1-\rho} \quad (8)$$

where

$$\beta = [1 - 4\rho(1-\rho)(1 - e^{2W/T})]^{1/2} \quad (9)$$

The pressure has the form

$$P/T = \ln\left\{ \frac{\rho}{1-\rho} \left[ \frac{(\beta + 1)(1-\rho)}{\beta + 1 - 2\rho} \right]^{c/2} \right\} \quad (10)$$

The critical parameters are

$$\rho_c = \frac{1}{2}; W/T_c = \ln(c/(c-2)) \quad (11)$$

The BG binodal equation is

$$t = \frac{2 \ln\left(\frac{c-2}{c}\right)}{-\ln(X)} \quad (12)$$

where

$$X = 1 + \frac{1}{4\rho(1-\rho)} \left[ \frac{(1+\chi)^2(1-2\rho)^2}{(1-\chi)^2} - 1 \right] \quad (13)$$

and

$$\chi(\rho, c) = \left( \frac{1-\rho}{\rho} \right)^{(2-c)/c} \quad (14)$$

For vanishing densities  $\rho \rightarrow 0$ , the eq 12 predicts

$$\rho = \frac{c-2}{c} \exp(-2/t) \quad (15)$$

An analytical expression for the Helmholtz energy of 3D Ising model has been obtained in ref 13 using a combination of statistical-mechanics and computer simulation methods. The analytical results of the binodal equation given in ref 12 were in good agreement with the numerical results of the Monte Carlo simulations of refs 10, 11. Both of these results are presented in Figure 1, where the corresponding binodals are plotted in reduced units ( $t, \rho$ ). The presented data are also in good agreement with the results of semianalytical theory given in ref 12. The shape of the BW and BG binodals is very steep. It is worth mentioning that the shape of binodals corresponding to theoretical results of ref 12 and the results of BG approach weakly depends on the number of the neighbor sites  $c$ . However, the BW predicted binodal is completely independent of the parameter  $c$ .

### III. Approximation of the Lattice Binodals

The BW and BG approximations give accurate results for thermodynamic properties, except the area close to critical point. According to eqs 5 and 11, the coexistence curve in the ( $\rho, t$ ) plane has following expression near the critical point ( $t = 1, \rho = 1/2$ ),

$$|\rho - 1/2| \sim (1 - t)^\beta \quad (16)$$

Here, the critical exponent has classical value  $\beta = 1/2$ . We note that the specificity of the exponent  $\beta$  near the critical point was not addressed in refs 10–13. Together with this, the value of this exponent obtained from numerical simulations in 3D space<sup>14</sup> does not match with classical value  $1/2$ . For example, the 3D Ising model gives  $\beta = 0.313$ , the 3D Heisenberg model provides  $\beta = 0.345$ . Thus, we suggest the following approximate expression for the lattice binodals with an arbitrary parameter  $\beta$

$$\rho = \frac{1}{2}(1 \pm (1 - e^{-(1-t^{1/\beta})/\beta t})^\beta) \quad (17)$$

The plus/minus signs here correspond to the liquid/gas branches of binodal. Applying a Taylor expansion to eq 17 near the critical point we arrive at eq 16. The gas density along the binodal at  $t \rightarrow 0$  has the following asymptotics

$$\rho = 0.5\beta \exp\left(-\frac{1}{\beta t}\right) \quad (18)$$

We see that eq 18 at  $\beta = 0.5$  coincides with eqs 6 and 15 with logarithmic accuracy. Therefore, the density exponentially decreases with temperature falls. Asymptotic form of eq 18 corresponds to the general dependence on temperature of gas density along the binodal at  $t \rightarrow 0$  for an arbitrary system.<sup>15</sup>

In the following, we use eq 17 to investigate the coexistence curves for different LM models. The binodals predicted by eq 17 are compared with the analytical results of Yan et al.,<sup>13</sup> and the simulation data of refs 10 and 11 in Figure 1. The two curves 4 and 5 in Figure 1 are calculated using eq 17 with  $\beta = 0.43$  and  $0.33$ , respectively. Curve 4 coincides with the binodals of refs 10–13 over the entire concentration range. Curve 5

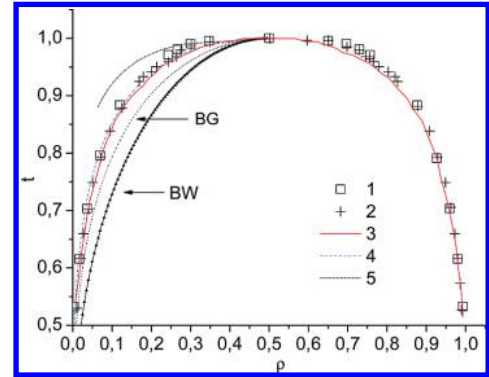


**Figure 1.** Comparison of coexistence curves of different lattice. Numerical calculations: 1, ref 10; 2, ref 11; 3, ref 13. Approximated models: BG, Bethe–Guggenheim approach ( $c = 6$ ) (ref 8); BW, Bragg–Williams approach (ref 9). The approximation used in this work (eq 17): 4,  $\beta = 0.43$ ; 5,  $\beta = 0.33$ .

**TABLE 1**

model	refs 10–13	BW (ref 8)	BG (ref 9)
$\beta$	0.43	0.48	0.55

describes with sufficient accuracy the near-critical region.<sup>10,11</sup> Unfortunately, no conclusive decision can be made on the basis of this comparison in the favor of the critical exponent  $\beta = 0.33$  due to its insufficient accuracy.

It should be noted that the eq 17 describes both the BW and BG models provided a proper value for the parameter  $\beta$  is chosen. We find that eq 17 has a potential to predict binodal lines with a very high accuracy over the entire density domain if the variable  $\beta$  is considered as a running parameter of the system. The calculated values for the critical exponent  $\beta$  are given in Table 1.

In the following section, we use eq 17 with fitting parameter  $\beta$  to describe the binodal line of a model system over the entire density domain.

### IV. Projective Transformation between the Lattice Variables and Liquid–Gas Variables

It was shown in ref 7 that a projective transformation maps the binodal of the LG onto the binodal of the real fluid. Such transformation creates a correspondence between the two triplets of three nonconcurrent lines<sup>16</sup> and thus considered to be unique. We propose a new projective transformation, which differs from the one used in ref 7. Our transformation has the form

$$n/n_B = \rho^\gamma / (1 + \alpha t); T/T_B = \alpha t / (1 + \alpha t) \quad (19)$$

Here, the temperature  $T_B$  corresponds to the Boyle point and  $n_B$  is the value of the density obtained by extrapolating the coexistence curve into the low temperature region beyond the triple point.<sup>2</sup> The parameters  $\alpha$  and  $\gamma$  are determined as

$$\alpha = T_c / (T_B - T_c); \gamma = \ln[n_c(1 + \alpha)/n_B] / \ln(1/2) \quad (20)$$

where  $T_c$  and  $n_c$  denote the critical temperature and density. The proposed transformation sets a new correspondence between two triplets of nonconcurrent lines in the plane ( $\rho, t$ ) for LM and plane ( $n, T$ ) for the real fluid. These two triplets are

$$t = 1 \Leftrightarrow T = T_c; \rho = \frac{1}{2} \Leftrightarrow n = n_c; \rho = 1 \Leftrightarrow n/n_B + T/T_B = 1 \quad (21)$$

We can see that the critical point ( $\rho = 1/2$ ,  $t = 1$ ) and Zeno-line of LM transform into the critical point ( $n_c$ ,  $T_c$ ), and the corresponding Zeno-line. In ref 7, the value of  $\gamma$  was equal to unity. In this case, the LM critical point is mapped onto the Zeno-median line. This is true only when the critical temperature and density in the plane ( $n$ ,  $T$ ) obey the relation  $2n_c/n_B + T_c/T_B = 1$  (Zeno-median). Further, we consider more general case in order to lift this restriction. The inverse transformation with respect to eq 19 becomes

$$\rho = \left[ \frac{n}{n_B(1 - T/T_B)} \right]^{1/\gamma}; t = \frac{1}{\alpha} \frac{T/T_B}{1 - T/T_B} \quad (22)$$

The applicability of this transformation is restricted by the inequality  $T < T_B$ . The substitution of these expression in Eqs.(5, 12) or 17 gives a transition from LM to continuous models or real substances.

It should be noted that after the substitution of transformation 22 into eq 17 the Zeno-line remains tangential to the liquid branch of the binodal at  $T \rightarrow 0$ . The expansion of the transformed binodal near the critical point has the following form:

$$n = n_c(1 + \alpha\tau) \left( 1 \pm \gamma \left( \frac{\alpha + 1}{\beta^2} \right)^\beta \tau^\beta + \dots \right) = n_c \left[ 1 + \alpha\tau \pm \gamma \left( \frac{\alpha + 1}{\beta^2} \right)^\beta \tau^\beta + \dots \right] \quad (23)$$

$$\tau = \frac{T_c - T}{T}, \tau \rightarrow 0$$

The positive sign in eq 23 corresponds to the liquid binodal branch of continuous liquid. One can see that the critical exponent of this binodal is exactly equal to  $\beta$ . Unless we consider  $\beta$  as a fitting parameter of our theory (and, of course, not necessarily  $\beta \approx 0.3$ ), we cannot expect that the transformation of eq 22 would correspond to the exact description of the critical domain. Aside from this, we have used in our previous works<sup>2–5</sup> another equation for the liquid branch of the binodal, which provided high accuracy both in the vicinity of the critical point and over the entire density range. The equation had Guggenheim's three-term form:<sup>6</sup>  $n = n_c + A\tau + B\tau^\beta$ , which is similar to eq 23 with different coefficients  $A$  and  $B$ . The value of the critical exponent was set as  $\beta = 0.33$  (or 0.5). The binodal equation we suggest in this work, despite of lacking high accuracy near the critical point, has a certain merit. It describes both liquid and gas branches of the coexistence curve over the entire density domain with acceptable accuracy.

## V. Binodal Transformation

We now consider the transformation 22 of the lattice binodal 17 into the binodal of a continuous system. As examples of the latter ones we chose the van der Waals and Lennard–Jones models, metals Cs and Hg, and ammonia. Below, we compare the results of calculations with the exact solution (vdW), numerical modeling (L–J) and experimental data (Cs, Hg, and NH<sub>3</sub>). The four parameters needed for the transformation are collected in Table 2.

TABLE 2

	vdW <sup>a</sup>	L–J <sup>a</sup>	Cs	Hg	NH <sub>3</sub>
$T_c$ , K	1	1.31	1938	1751	405.4
$n_c$ , g/cm <sup>3</sup>	1	0.314	0.39	5.8	0.225
$T_B$ , K	27/8	3.418	3500	6350	955.9
$n_B$ , g/cm <sup>3</sup>	3	1.14	1.96	14.4	0.95
$\beta$	0.59	0.434	0.546	0.464	0.456
$\epsilon_{\text{Liq}}$ , %	3.076	11.92	5.418	5.475	4.983

<sup>a</sup> We use dimensionless units reduced to the critical point for the van der Waals equation and Lennard–Jones units for the Lennard–Jones system. For Cs, Hg, and NH<sub>3</sub>, the density and temperature are expressed in g/cm<sup>3</sup> and K, respectively.

The comparison of experimentally defined binodals for models and substances from Table 2 is given in Figure 2. Figure 2 also contains coexisting lines calculated from the transformation of lattice models (TLM). Again, the region of critical point has a lesser accuracy as a result of the transformation 22. However, the liquid branch of the binodal has acceptable accuracy as shown in Table 2. We also present in Table 2 optimal values for exponent  $\beta$  and the maximal value of the density error defined as  $\epsilon_{\text{Liq}} = \max_T |1 - n_{\text{calcd}}(T)/n_{\text{exact}}(T)|$  along the liquid branch of the binodal. The density error for the gas binodal branch is smaller than the density error for the liquid branch excluding only the region of extremely small densities  $n \rightarrow 0$ , where the ratio  $n_{\text{calcd}}(T)/n_{\text{exact}}(T)$  becomes indeterminate.

## VI. Critical Isotherm Transformation

There is no straightaway method to use the technique suggested in previous section to construct an equation of state for the nonlattice model system and real substances in the liquid–gas part of the phase diagram. For this purpose, we may use the pressure expression derived for some lattice model and then perform the transformation 22 from the lattice variables ( $\rho$ ,  $t$ ) to the ordinary thermodynamic variables ( $n$ ,  $T$ ). Let us prove the validity of such suggestion for the van der Waals equation. The three pressure isotherms according to the van der Waals equation at  $T = T_c$ ,  $T = 1.1T_c$  and  $T = 0.9T_c$  are presented in Figure 3 together with corresponding TLM isotherms of the BG and BW approaches. As it is clear from Figure 3, the difference between the BG and BW results is negligible. It also follows from Figure 3 that the difference between the critical isotherms is small as well. It becomes noticeable only at  $1/\text{density} > 2$ . However, the difference between noncritical isotherms is not small. We therefore conclude that 1) the LM transformation has the greatest accuracy for the critical isotherm, 2) the accuracy decreases as one moves away from the critical temperature. To check the first statement, we calculate the pressure along the critical isotherms for the same model systems and real substances listed above, using eqs 5 and 10 for the BW and BG lattice models and the transformation of eq 22. Obtained results are presented in Figure 4. The TLM isotherms describe pretty well the results of numerical modeling<sup>17,18</sup> for the Lennard–Jones system (part “a” of Figure 4). The TLM isotherms reproduce the isotherms of real substances Cs (part “b” of Figure 4), Hg (part “c” of Figure 4), and NH<sub>3</sub> (part “d” of Figure 4) quite well too. The deviation of the experimental (or numerical) isotherms from the TML isotherms at their horizontal part does not exceed several percent. The best agreement over the entire density domain takes place for ammonia.

The calculated TLM isotherms for metals are steep curves at small specific volume ( $1/n$ ) values in comparison with the experimental curves. The reason for this discrepancy is not clear



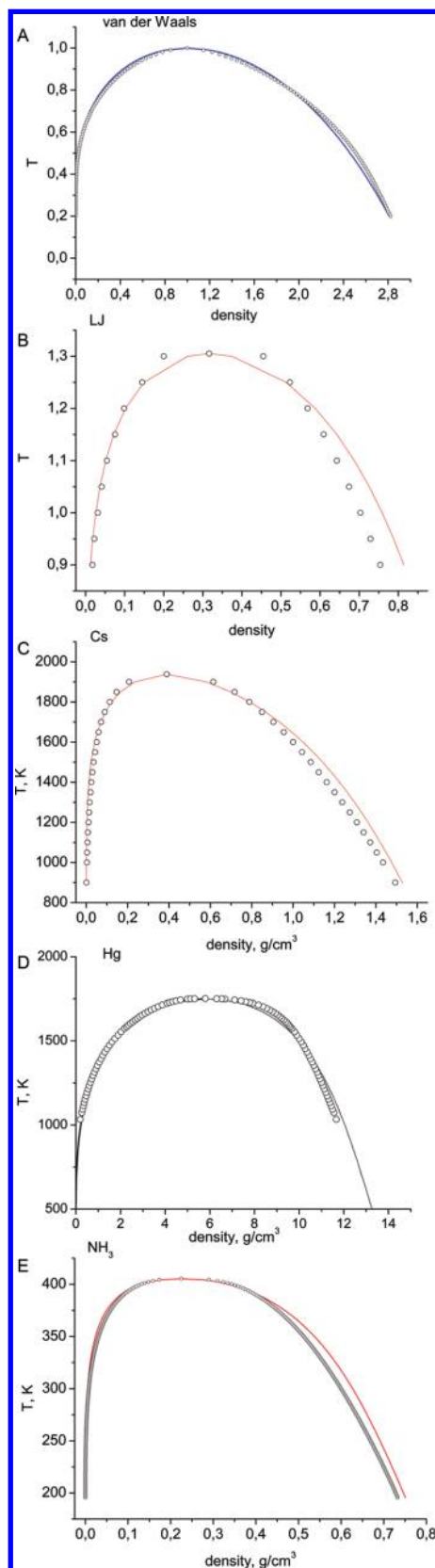


**Figure 2.** Comparison of binodal curves predicted by numerical simulations and obtained in experimental works with the binodal curves resulting from the transformation of lattice binodals (TLB): a) the van der Waals equation: the symbols correspond to the exact solution of this equation, solid curve is TLB with  $\beta = 0.59$ ; b) the Lennard–Jones system: points are for numerical simulations of ref 17 solid curve is the TLB; c), d), and e) cases for cesium, mercury, ammonia, respectively: the points are for the experimental results of refs 19–21, solid curves are the TLB method.

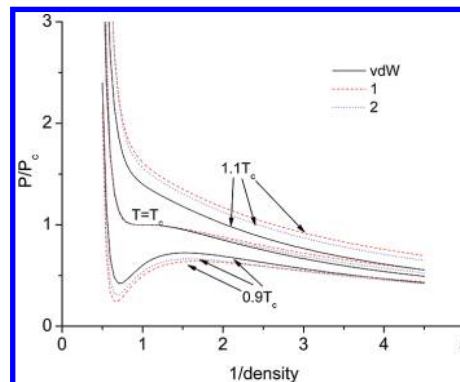


**Figure 3.** Comparison the pressure isotherms according to the van der Waals equation (vdW) with isotherms resulting from the transformation of lattice models: Lines 1, BG with  $c = 6$  (ref 8); Lines 2, BW (ref 9) at  $T = T_c$ ;  $T = 1.1T_c$  and  $T = 0.9T_c$ .

and might be attributed to the errors in the experimental data and calculated parameters ( $n_c$ ,  $T_c$ ,  $n_B$ , and  $T_B$ ).

We also note that for organic substances it is possible to apply the lattice fluid theory to the continuous liquid at  $T \leq T_c$  and get the thermodynamic values with high accuracy.<sup>21</sup> But this approach relies on a semianalytical expression for Helmholtz energy with parameter fitting for every particular substance.

## VII. Discussion of Thermodynamic Similarity

In the previous section, we have shown that thermodynamical properties of the LM model have a weak dependence on the LM lattice parameter. As a result of this fact, the transformations 17 and 22 contain only two parameters defined by the properties of real matter. These parameters are  $a = n_c/n_B$  and  $\alpha = T_c/(T_B - T_c)$ . The first parameter determines the position of the critical density in the  $(n, T)$  plane. The second parameter defines the binodal opening.<sup>4</sup> Both parameters are well explored for different materials: the mercury has  $a = 0.4$ ,  $\alpha = 0.369$ , and the cesium has  $a = 0.2$ ,  $\alpha = 0.887$ . As it is known from literature, mercury has the smallest binodal opening among classical liquids; however, cesium has the widest binodal opening. It is anticipated that substances with closest parameters  $a$  and  $\alpha$  also have thermodynamically similar features. The calculated values of  $n_c/n_B$  and  $T_c/T_B$  are given in Table 1 of ref 4 (which is not shown here). Using available data from ref 4, we determine the parameter  $\alpha = T_c/(T_B - T_c)$ . We also check whether the values of  $a$  and  $\alpha$  for a group of substances with similar thermodynamic properties are the same.

Obtained results, given in Table 3, clearly show that the parameter  $a = n_c/n_B$  has nearly the same value for all considered substances. However, this not the case for the binodal opening parameter  $\alpha$ , which has a wide range of variations.

It should be noted that some refined thermodynamic properties of investigated systems have no dependence on the value of  $a - \alpha$  parameters. For example, whereas many alkali metals and Hg have similar  $a$  and  $\alpha$  parameters, they show a deviation from the law of rectilinear diameter near the critical point (see refs., 7 19, and 20). Such deviation is due to peculiarities of electronic structure of these metals and, apparently, is not connected with the  $a - \alpha$  values.

It should be noted that nonalkali metals (Al, Cu, W, U, Zr) considered earlier in ref 4 have  $\alpha > 0.8$  too, whereas the other nonmetallic substances have  $\alpha < 0.8$ . So, in Table 3 there is a column metal combining the alkali and nonalkali metals. Exclusion is only for Hg, which is “bad” metal (ref 20). So, it is possibly that the value of  $\alpha \approx 0.8$  can separate conducting

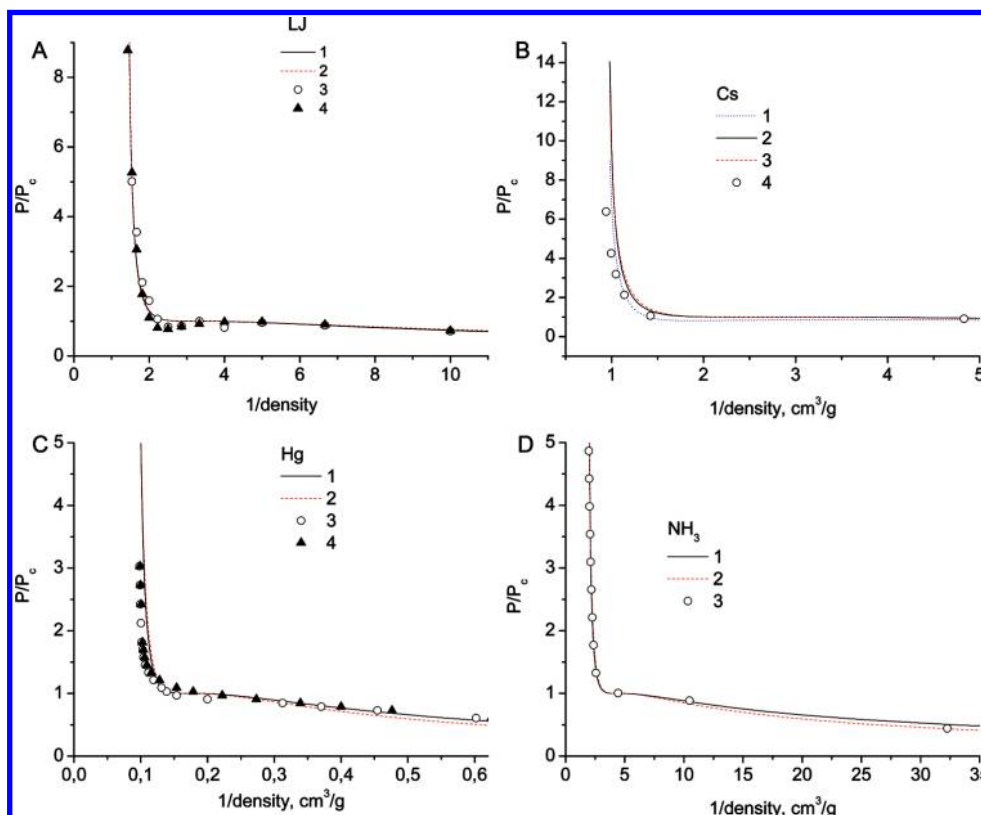


**Figure 4.** Dependence of the pressure along the critical isotherms for the model system and real substances: a) Lennard–Jones system: 1, BG with  $c = 6$ ; 2, BW; 3, ref 17; 4, ref 18. b) Cesium: 1, BG isotherm at  $T = 1900$  K; 2, BG critical isotherm with  $c = 6$ ; 3, BW critical isotherm; 4, experimental isotherm of ref 19 at  $T = 1900$  K. c) mercury: 1, with  $c = 6$ ; 2, BW; 3 and 4 are the experimental isotherms of ref 20 with  $T = 1748$  K and  $1773$  K, respectively. d) Ammonia: 1, BG with  $c = 6$ ; 2, BW; 3, experiment of ref 21.

**TABLE 3: Calculated Values of Parameters  $a$  and  $\alpha$  for Different Substances**

substances and models	noble and molecular gases (Ar, Xe, Kr, Ne, F <sub>2</sub> , O <sub>2</sub> , N <sub>2</sub> )	organic and polar fluids (CH <sub>4</sub> , C <sub>2</sub> H <sub>6</sub> , C <sub>2</sub> H <sub>4</sub> , C <sub>6</sub> H <sub>14</sub> , etc., CO <sub>2</sub> , NH <sub>3</sub> )	metals (K, Cs, Rb, Na, Li, Al, Cu, W, U, Zr)	L–J system	water	mercury
parameter $\alpha$	0.587–0.639	0.6130.613–0.754	0.8–1.0	0.613	1.04	0.369
parameter $a$	0.27–0.30	0.24–0.29	0.15–0.25	0.285	0.27	0.4

(not only metals) and nonconducting substances. But this issue demands further investigation as well as any other particular connection between thermodynamic property and pair  $a - \alpha$ .

## VIII. Conclusions

In this work, a new step is made toward the better understanding of the similarity relations between the thermodynamics of lattice models and real substances. We have shown that the lattice binodals and critical isotherms transforms with sufficient accuracy into binodals and critical isotherms of real substances (Cs, Hg, and NH<sub>3</sub>) or model systems reflecting properties of real matter (the van der Waals equation, Lennard–Jones system). The expression for critical isotherm obtained in this work can be used to test the accuracy of equations of state proposed by different models near the critical point. Using the equation of state, it is possible to calculate the pressure along the critical isotherm, taking the difference between the thermal and potential parts of pressure. Both of these parts usually have the same magnitude, making the resulting pressure very small with little precision. Simulation results of ref 23 for an L–J system near the critical point  $T_c = 1.35$ ,  $\rho_c = 0.35$  show that the thermal and potential parts of pressure are 109.42 and 109.28 correspondingly, leading to small critical point pressure  $P_c = 0.14$ . This circumstance demands high accuracy from usual

equations of state. However, the method of the critical isotherm calculation suggested in the current work is completely free from such a drawback.

We express gratitude to Liu Honglai for additional information concerning works of refs 13 and 22. This study was supported by the Russian Foundation for Basic Research under Grant Nos. 09–03–00081a and 08–08–00351a.

## References and Notes

- (1) Hill, T. *Statistical Mechanics*; Mc-Graw-Hill, 1956.
- (2) Apfelbaum, E. M.; Vorob'ev, V. S. *J. Phys. Chem. B* **2008**, *112*, 13064.
- (3) Apfelbaum, E. M.; Vorob'ev, V. S. *Chem. Phys. Lett.* **2009**, *467*, 318.
- (4) Apfelbaum, E. M.; Vorob'ev, V. S. *J. Phys. Chem. B* **2009**, *113*, 3521.
- (5) Apfelbaum, E. M.; Vorob'ev, V. S. *J. Chem. Phys.* **2009**, *130*, 214111.
- (6) Guggenheim, E. A. *J. Chem. Phys.* **1945**, *13*, 253.
- (7) Kulinskii, V. L. *J. Phys. Chem. B* **2010**, *114*, 2852.
- (8) Bragg, W. L.; Williams, E. J. *Proc. Roy. Soc. A* **1934**, *145*, 699.
- (9) Guggenheim, E. A. *Mixtures*; Oxford University Press: London, 1952.
- (10) Yan, Q. L.; Liu, H. L.; Hu, Y. *East China Univ. Sci. Techn.* **1996**, *22*, 188. in Chinese.
- (11) Zweistra, H. J.; A. Besseling, N. A. M. *Phys. Rev. E* **2006**, *74*, 016111.
- (12) Panagiotopoulos, A. Z. *J. Chem. Phys.* **2000**, *112*, 7132.

- (13) Yan, Q.; Liu, H.; Hu, Y. *Fluid Phase Equilib.* **2004**, 218, 157.
- (14) Balescu, R. *Equilibrium and Nonequilibrium Statistical Mechanics*; Wiley Interscience Publications: John Wiley and Sons, 1975.
- (15) Landau, L. D.; Lifshitz, E. M. *Statistical Physics*; Pergamon: Oxford, 1980.
- (16) Hartshorne, R. *Foundations of Projective Geometry*; Addison-Wesley Publishing Co.: Reading, MA, 1968.
- (17) Ou-Yang, W. Z.; Lu, Z.-Y.; Shi, T.-F.; Sun, Z.-Y.; An, L.-J. *J. Chem. Phys.* **2005**, 123, 254502.
- (18) Mecke, M.; Muller, A.; Winkelmann, J.; Vrabec, J.; Fischer, J.; Span, R.; Wagner, W. *Int. J. Thermophysics* **1996**, 17, 391.
- (19) Kozhevnikov, V. F. *Sov. Phys. JETP (in Russian)* **1990**, 97, 541.
- (20) Kikoin, I. K.; Sencenkov, A. P. *Phys. Met. Metallography. (Fizika metallov i metallovedenie (in Russian))* **1967**, 24, 843.
- (21) Lemmon, E. W.; McLinden, M. O.; Friend, D. G. *Thermophysical Properties of Fluid Systems. In NIST Chemistry WebBook, NIST Standard Reference Database Number 69 [Online]*; Linstrom, P. J., Mallard, W. G., Eds.; National Institute of Standards and Technology.
- (22) Xu, X.; Liu, H.; Peng, C.; Hu, Y. *Fluid Phase Equilib.* **2008**, 265, 112.
- (23) Nicolas, J. J.; Gubbins, K. E.; Streett, W. B.; Tildesley, D. J. *Mol. Phys.* **1979**, 37, 1429.

JP1022899